

Numerical Investigation of Heat Transfer and Fluid Flow Characteristics Inside Wavy Channels Fully Filled With Porous Media

Fahad Sabah Al-Gburi¹ & Amir Sultan Dawood¹

¹ Mechanical Engineering Department, Collage of Engineering, Mosul University, Mosul, Iraq

Correspondence: Fahad Sabah Al-Gburi, Mechanical Engineering Department, Mosul University, Mosul, Iraq.
Tel: 964-770-278-2918. E-mail: fahad_sabah2001@yahoo.com, fahadsabah88@gmail.com

Received: May 20, 2013 Accepted: June 24, 2013 Online Published: July 15, 2013

doi:10.5539/mer.v3n2p13 URL: <http://dx.doi.org/10.5539/mer.v3n2p13>

Abstract

The combined effect of waviness and porous media on the convection heat transfer and fluid flow characteristics is numerically investigated. Two models of wavy walled channel fully filled with homogenous porous material are assumed. The first was the symmetric converging-diverging channel (case A), and the second was the channel with concave-convex walls (case B). The governing equations have been solved on non-orthogonal grid, which is generated by Poisson elliptic equations, based on ADI method. Nusselt number values are used to indicate whether any cases of corrugation studied may have led to an increase in the rate of heat transferred compared with the planar surface channel which is the purpose of the study. The results show that case A gives more enhancement in heat transfer than case B. However, the thermal performance of the wavy channels (cases A & B) is better than the straight channel (simple duct).

Keywords: porous media, wavy channels, separation, elliptic grid generation, forced convection, non-darcian flow

Nomenclature

c_p	Specific heat, $J \cdot kg^{-1} \cdot K$
Da	Darcy number
F	Form-drag constant
H	Channel width (characteristic length), m
h	Wavy amplitude, m
k	Thermal conductivity, $W \cdot m^{-1} \cdot K^{-1}$
K	Permeability of porous medium, m^2
Nu_x	Local Nusselt number
Nu	Average Nusselt Number
p	Pressure, Pa
Pr	Prandtl number
Re	Reynolds number
T	Temperature, K
u	Horizontal velocity component, $m \cdot s^{-1}$
u_0	Inlet velocity, $m \cdot s^{-1}$
v	Vertical velocity component, $m \cdot s^{-1}$
$ V $	Velocity magnitude = $(u^2 + v^2)^{0.5}$, $m \cdot s^{-1}$

Greek symbols

α	Thermal diffusivity, $m^2 \cdot s^{-1}$
θ	Dimensionless temperature
μ	Dynamic viscosity, $Pa \cdot s$
ν	Kinematic viscosity, $m^2 \cdot s^{-1}$
ξ, η	Computational region coordinates
ρ	Density, $kg \cdot m^3$
ϕ	Porosity of porous medium
ψ	Stream function, $m^2 \cdot s^{-1}$
ω	Vorticity, s^{-1}

Subscripts

f	fluid
h	Hot surface
in	Inlet condition

Accents

\hat{t}	Non-dimensional
-----------	-----------------

1. Introduction

Heat and mass transfer through porous media is an important development and an area of very rapid growth in contemporary heat transfer researches; because of its existence in many diverse applications such as ground-water hydrology, production of oil and gas from geological structures, the gasification of coal, geothermal operations, packed-bed chemical reactors, surface catalysis of chemical reactions, filtration, adsorption, drying, compact heat exchangers and many more. Many researchers interested with enhancing heat transfer rate by using porous media. Hadim and North (2005) presented a numerical investigation of two-dimensional laminar forced convection in a sintered porous channel with inlet and outlet slots. They studied the effects of the particle diameter, particle Reynolds number, and channel dimensions on flow and heat transfer. They developed length-averaged Nusselt number and friction factor correlations for efficient design of a porous metal heat exchanger. Mohammad (2003) numerically investigated heat transfer enhancement for a flow in a pipe and a channel fully or partially filled with porous medium. The effects of porous layer thickness on the rate of heat transfer and pressure drop were investigated. He mentioned that partially filling the conduit with porous medium enhances the rate of heat transfer. Van der Sman (2002) tested the validity of the Darcy-Forchheimer-Brinkman (DFB) theory of flow through confined porous media using experimental data of pressure drop and velocity correlations which are describing the airflow through a vented box packed with horticultural produce. His Results show that the DFB model can reproduce experimental data on pressure drop quite accurately. Angirasa (2002) presented an experimental investigation to demonstrate the heat transfer enhancement with metallic fibrous heat dissipaters. He concluded that the metallic porous heat dissipaters can achieve substantial heat transfer augmentation when compared to flat plate. Kim et al. (2001) presented an experimental study to investigate the impact of the presence of aluminum foam on the flow and convective heat transfer in an asymmetrically heated channel. They presented a simple correlation of the friction factor and the average Nusselt number of aluminum foams will be sought to provide a guide in practical applications. Kaviany (1985) developed a numerical work to investigate the fluid flow and heat transfer characteristics due to laminar flow between two isothermal parallel plates. His results show that Nusselt number for fully-developed fields increases with an increase in porous media inside the channel, while the pressure drop associated with the entrance region decreases. Vafai and Tien (1981) numerically analyzed the effects of the solid boundary and the inertial forces on flow and heat transfer in porous media attached over flat plate. Their results show that these effects are more pronounced in highly permeable media, high Prandtl number, large pressure gradients, and in the region close to the leading edge of the flow layer.

The geometrical shape of the channel walls is also one of great importance in enhancing heat transfer. The waviness is a special case of corrugation that can be used to promote heat transfer. Xei et al. (2007) numerically studied the effects of wavy heights, lengths, wavy pitches and channel widths of a wavy channel on fluid flow and heat transfer characteristics. The results showed that the heat transfer may be greatly enhanced due to the wavy characteristics. Wang and Chen (2002) had numerically studied the effects of the wavy geometry, Reynolds number and Prandtl number on the skin-friction and Nusselt number for flow through a sinusoidal curved converging-diverging channel. Their results showed that the amplitudes of Nusselt number and the skin-friction coefficient curves increase as Reynolds number and the amplitude-wavelength ratio increase. Russ and Beer (1997a, 1997b) numerically and experimentally studied the heat and mass transfer for a wide range of Reynolds numbers from laminar to turbulent flow in a pipe of a wavy surface. Their results showed that frictional loss increases with the increase of amplitude for the same Reynolds number. Moreover, a maximum value of Nusselt number was determined near the reattachment point of the flow in the converging part of the wave. Tanda and Vittori (1996) presented a numerical study for fully developed flow and heat transfer in a wavy channel. Their results showed that The position of the local heat transfer coefficient is sensitive to Reynolds and Prandtl numbers and to the geometric parameters of the wall waviness. Stone and Vanka (1996) have presented an accurate numerical scheme to solve the unsteady flow and heat transfer equations in a wavy passage. They observed that the flow is steady in part of the channel and unsteady in the rest of it. Also, as Reynolds number is progressively increased, the unsteadiness is onset at a much earlier location, accompanied by increased overall heat transfer and friction coefficients. Saniei and Dini (1993) experimentally studied the heat transfer characteristics due to turbulent flow conditions in a wavy-wall channel containing from seven waves. They concluded that the local Nusselt number has the highest magnitude on the second wave.

Based on the reported importance of using porous media in a hand, and using corrugated surfaces on the other hand, in improving and increasing the heat transfer, the present work integrates these two ideas and numerically investigates their combined effect on the nature of the flow and heat transfer by forced convection. So, this study assumed two models of wavy walled channel, fully filled with homogenous porous material. The first was the

symmetric converging-diverging channel (case A), and the second was the channel with concave-convex walls (case B) (see Figure 1). Nusselt number values are used to indicate whether any cases of corrugation studied may have led to an increase in the rate of heat transferred compared with the planar surface channel which is the purpose of the study.

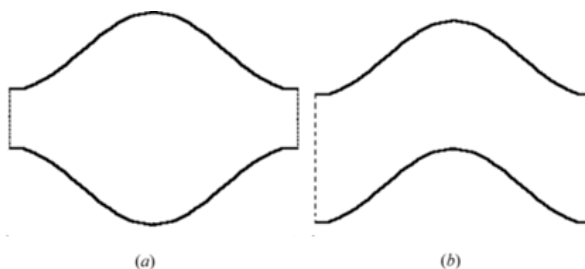


Figure 1. Models of wavy channels. (a) Symmetric converging-diverging channel, (b) Channel with concave-convex walls

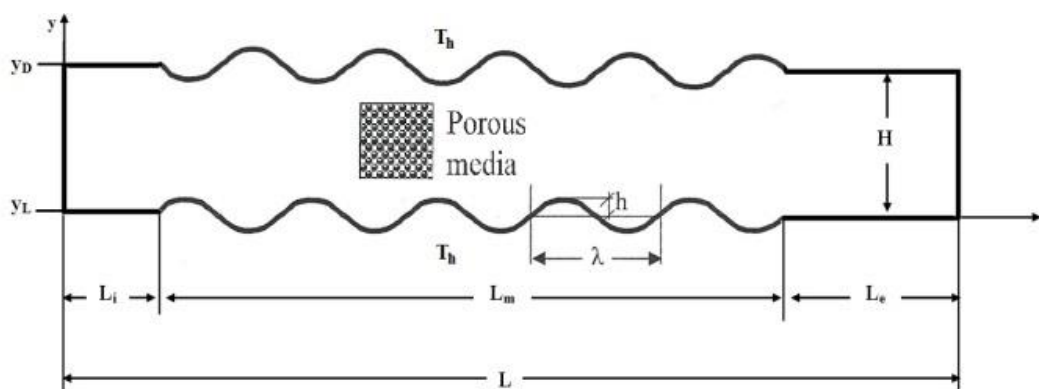


Figure 2. Schematic configuration of the physical model of the present study

2. Mathematical Formulation

In this study, a schematic configuration of the physical model, which is a two-dimensional wavy channel, is illustrated in Figure 2. This channel is completely filled with porous material and divided into three regions. The first is the entrance region of length ($L_i = 10H$), the second is the wavy-walled region of length ($L_m = 10H$) whereas the last is the exit region of length ($L_e = 5H$). The following equations respectively define the coordinates of the upper and lower surfaces:

$$y_L = \begin{cases} 0 & x \leq L_i \\ h \cdot \sin \frac{2\pi(x-L_i)}{\lambda} & L_i \leq x \leq L_i + L_m \\ 0 & x \geq L_i + L_m \end{cases} \quad (1)$$

$$y_D = \begin{cases} H & x \leq L_i \\ H \pm y_L & L_i \leq x \leq L_i + L_m \\ H & x \geq L_i + L_m \end{cases} \quad (2)$$

Where h and λ have a constant values in the current study for the two models (A & B). Their values are ($h = 0.25H$) and ($\lambda = 5/3H$) respectively.

This study considered steady state, incompressible, laminar, and two-dimensional flow. Also, it assumed homogeneous and isotropic sintered porous medium. The minimal temperature is that of the fluid at the inlet section (T_i), whereas the maximal one is of the channel walls (T_h). The fluid and the solid matrix are in local thermal equilibrium and viscous dissipation was neglected. The thermo-physical properties are assumed to be constant for the fluid (air) and the solid matrix.

According to the above considerations and assumptions, the governing equations will be as the followings (Vafai & Tien, 1981):

Continuity

$$\frac{\partial u}{\partial x} + \frac{\partial v}{\partial y} = 0 \quad (3)$$

Momentum

$$\frac{\rho_f}{\phi^2} \left(u \frac{\partial u}{\partial x} + v \frac{\partial u}{\partial y} \right) = -\frac{\partial p}{\partial x} - \frac{\mu_f}{K} u - \frac{\rho_f \cdot F}{\sqrt{K}} \sqrt{u^2 + v^2} \cdot u + \frac{\mu_f}{\phi} \left(\frac{\partial^2 u}{\partial x^2} + \frac{\partial^2 u}{\partial y^2} \right) \quad (4)$$

and

$$\frac{\rho_f}{\phi^2} \left(u \frac{\partial v}{\partial x} + v \frac{\partial v}{\partial y} \right) = -\frac{\partial p}{\partial y} - \frac{\mu_f}{K} v - \frac{\rho_f \cdot F}{\sqrt{K}} \sqrt{u^2 + v^2} \cdot v + \frac{\mu_f}{\phi} \left(\frac{\partial^2 v}{\partial x^2} + \frac{\partial^2 v}{\partial y^2} \right) \quad (5)$$

Energy

$$u \cdot \frac{\partial T}{\partial x} + v \frac{\partial T}{\partial y} = \alpha_f \cdot \left[\frac{\partial^2 T}{\partial x^2} + \frac{\partial^2 T}{\partial y^2} \right] \quad (6)$$

Where K and ϕ are the permeability and porosity of the porous structure, and F is a dimensionless form-drag constant, which is evaluated by using the widely used empirical correlation (Hadim & North, 2005):

$$F = \frac{1.75}{\sqrt{150} \phi^{1.5}} \quad (7)$$

The dimensionless forms have been rendered for the quantities with respect to the characteristic length (H), and the characteristic velocity (u_o) as the following:

$$\hat{x} = \frac{x}{H}, \hat{y} = \frac{y}{H}, \theta = \frac{T - T_i}{T_h - T_i}, \hat{u} = \frac{u}{u_o}, \hat{v} = \frac{v}{u_o},$$

$$\hat{p} = \frac{p}{\rho_f u_o^2}, Pr = \frac{\mu_f c_{p_f}}{k_f}, Re = \frac{u_o H}{\nu_f}, Da = \frac{K}{H^2} \quad (8)$$

In this study, the pressure terms in Equations (4) and (5) had been eliminated by differentiating these equations with respect to y and x respectively, and then subtracting one of them from the other. By using the dimensionless groups (8), the following equations will be the final form of the governing equations in terms of vorticity-stream function formula:

$$\hat{\omega} = -\hat{\nabla}^2 \hat{\psi} \quad (9)$$

$$\frac{1}{\phi} \left[\hat{u} \cdot \frac{\partial \hat{\omega}}{\partial \hat{x}} + \hat{v} \frac{\partial \hat{\omega}}{\partial \hat{y}} \right] = \frac{1}{Re} \hat{\nabla}^2 \hat{\omega} - \frac{\phi}{Re Da} \cdot \hat{\omega} - \frac{\phi F}{\sqrt{Da}} |\hat{V}| \omega + \frac{\phi F}{\sqrt{Da}} \left[\hat{u} \frac{\partial |\hat{V}|}{\partial \hat{y}} - \hat{v} \frac{\partial |\hat{V}|}{\partial \hat{x}} \right] \quad (10)$$

$$\hat{u} \frac{\partial \theta}{\partial \hat{x}} + \hat{v} \frac{\partial \theta}{\partial \hat{y}} = \frac{1}{Re \cdot Pr} \hat{\nabla}^2 \theta \quad (11)$$

Where

$$\hat{u} = \frac{\partial \hat{\psi}}{\partial \hat{y}}, \hat{v} = -\frac{\partial \hat{\psi}}{\partial \hat{x}} \quad (12)$$

The boundary conditions must be specified to solve the partial differential equations, which govern the model of study. No slip condition is considered at the solid walls (top and bottom). The flow over the cross-section at the inlet of the channel has uniform velocity (u_o), whereas at the outlet section is fully developed. Thus, the dimensionless boundary conditions will be:

1) At the inlet section:

$$\hat{u} = \hat{u}_o = 1, \hat{v} = 0, \hat{\psi} = \hat{u}_o \cdot \hat{y} = \hat{y}, \hat{\omega} = 0, \theta = 0$$

2) At the outlet section:

$$\frac{\partial \hat{u}}{\partial \hat{x}} = 0, \quad \hat{v} = 0, \quad \frac{\partial \hat{\psi}}{\partial \hat{x}} = 0, \quad \frac{\partial \hat{\omega}}{\partial \hat{x}} = 0, \quad \frac{\partial \theta}{\partial \hat{x}} = 0$$

3) At the bottom wall:

$$\hat{u} = 0, \quad \hat{v} = 0, \quad \hat{\psi} = 0, \quad \hat{\omega} = \frac{\partial^2 \hat{\psi}}{\partial \hat{n}^2}, \quad \theta = 1$$

4) At the top wall:

$$\hat{u} = 0, \quad \hat{v} = 0, \quad \hat{\psi} = \hat{u}_0 \cdot H = 1, \quad \hat{\omega} = \frac{\partial^2 \hat{\psi}}{\partial \hat{n}^2}, \quad \theta = 1$$

In order to manage the irregular boundaries in the model (wavy walls), it is important to assume new coordinates (ξ, η) , which introduce a regular domain, instead of the original coordinates (x, y) . The general transformation from the physical domain (x, y) to the computational domain (ξ, η) is:

$$\xi = \xi(x, y), \quad \eta = \eta(x, y) \quad (13)$$

The governing equations are solved on a curvilinear non-orthogonal grid, which is generated by solving Poisson's elliptic equation system. This system is represented by the following two equations:

$$\xi_{xx} + \xi_{yy} = P(\xi, \eta) \quad (14)$$

$$\eta_{xx} + \eta_{yy} = Q(\xi, \eta) \quad (15)$$

Middlecoff and Thomas (1980) developed a method to evaluate the values of the control functions (P) and (Q) by assuming the following :

$$P = \Phi(\xi, \eta) (\xi_x^2 + \xi_y^2) \quad (16)$$

$$Q = \Psi(\xi, \eta) (\eta_x^2 + \eta_y^2) \quad (17)$$

Where the parameters Φ and Ψ are evaluated as follows:

$$\Phi = - \left. \frac{\hat{x}_{\xi\xi} \hat{x}_\xi + \hat{y}_{\xi\xi} \hat{y}_\xi}{\hat{x}_\xi^2 + \hat{y}_\xi^2} \right|_{\eta=\eta_b} \quad (18)$$

$$\Psi = - \left. \frac{\hat{x}_{\eta\eta} \hat{x}_\eta + \hat{y}_{\eta\eta} \hat{y}_\eta}{\hat{x}_\eta^2 + \hat{y}_\eta^2} \right|_{\xi=\xi_b} \quad (19)$$

Where η_b and ξ_b respectively are the values of η and ξ along the boundaries.

Upon introducing terms P and Q from Equations (16, 17), after specifying the parameters (Φ, Ψ) , the transformed form of Equations (14, 15) will be as the following:

$$\alpha(\hat{x}_{\xi\xi} + \Phi \hat{x}_\xi) - 2\beta \hat{x}_{\xi\eta} + \gamma(\hat{x}_{\eta\eta} + \Psi \hat{x}_\eta) = 0 \quad (20)$$

$$\alpha(\hat{y}_{\xi\xi} + \Phi \hat{y}_\xi) - 2\beta \hat{y}_{\xi\eta} + \gamma(\hat{y}_{\eta\eta} + \Psi \hat{y}_\eta) = 0 \quad (21)$$

Where

$$\alpha = \hat{x}_\eta^2 + \hat{y}_\eta^2 \quad (22)$$

$$\beta = \hat{x}_\xi \hat{x}_\eta + \hat{y}_\xi \hat{y}_\eta \quad (23)$$

$$\gamma = \hat{x}_\xi^2 + \hat{y}_\xi^2 \quad (24)$$

By solving the Equation systems (20, 21) numerically using Line successive over relaxation (LSOR) method (Petrović & Stupar, 1996), a typical grid system would be generated for the posed model like the illustrated in Figure 3. It is important to mention that suitable clustering functions were used in mesh generation operation in order to increase the density of the grid points in the regions having high steeper gradients (Petrović & Stupar, 1996) like the furrows of the wavy surfaces.

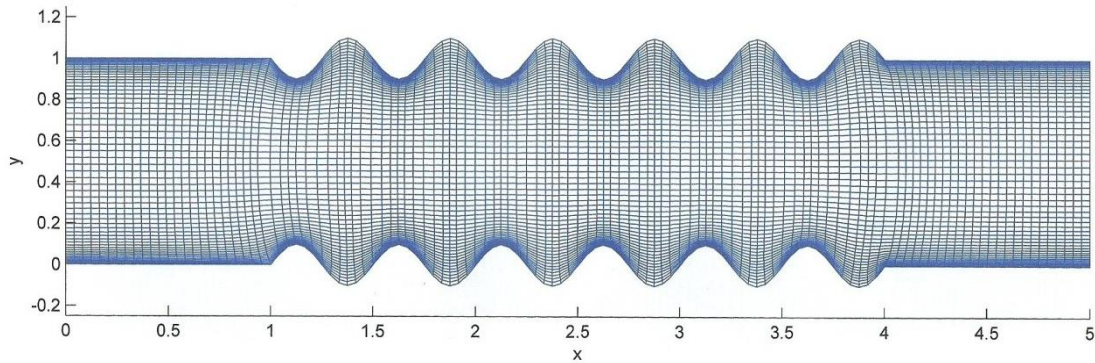


Figure 3. Poisson's elliptic grid of the present study

The local Nusselt number along the top and bottom surfaces is defined as follow:

$$Nu_{\hat{x}} = - \frac{\partial \theta}{\partial \hat{n}} \frac{1}{1 - \theta_b} \quad (25)$$

Where θ_b is dimensionless bulk temperature of flow inside the channel, which can be defined as follows:

$$\theta_b = \frac{\int_{\hat{y}_L}^{\hat{y}_D} \hat{u} \cdot \theta \cdot d\hat{y}}{\int_{\hat{y}_L}^{\hat{y}_D} \hat{u} \cdot d\hat{y}} \quad (26)$$

So, the local Nusselt number in the computational domain will be:

$$Nu_{\hat{x}} = - \frac{\sqrt{\gamma}}{J(1 - \theta_b)} \frac{\partial \theta}{\partial \eta} \quad (27)$$

Where J denotes the Jacobian of the transformation

$$J = J \left[\begin{matrix} \hat{x}, \hat{y} \\ \xi, \eta \end{matrix} \right] = \hat{x}_\xi \hat{y}_\eta - \hat{x}_\eta \hat{y}_\xi \quad (28)$$

From Equation (23), the average Nusselt number between any two positions at the surfaces of the channel is defined as:

$$Nu = \frac{\int_{\xi_1}^{\xi_2} \frac{Nu_{\hat{x}}}{J} \sqrt{\gamma} \cdot d\xi}{\int_{\xi_1}^{\xi_2} \frac{1}{J} \sqrt{\gamma} \cdot d\xi} \quad (29)$$

3. Numerical Procedure

3.1 Numerical Solution

Finite differences techniques with second-order of approximation were used to solve the governing Equations (9-11), with specified boundary conditions, after transforming these equations from its original form in (\hat{x}, \hat{y}) coordinates to (ξ, η) coordinates. The linear algebraic equations resulting from the finite differences techniques were solved using the alternating direction implicit method (ADI) with relaxation factor (Petrović & Stupar, 1996), which is one of the iterative methods. The values of the relaxation factor are evaluated by trial and error, and its values were between (0.7-0.9).

The grid size was of great importance in the validity of the results. Grid independence was verified, by running several different grid sets (60×350 , 80×380 and 100×400) and by testing its effect on Nusselt number, to observe less than 2% difference between ($60 \times 350, 100 \times 400$) grid sets. Thus, the grid size (60×350) was performed for all runs. The convergence criterion (maximum relative error in the values of the dependent variables between two successive iterations) in all runs was set at 10^{-6} . Typically, 4000 iterations were required for the local variables (Temperature, stream function, and vorticity) to achieve the set convergence. The results are generated by the developed Matlab code (M-file).

3.2 Code Validation

In order to test the accuracy and validity of the numerical procedure, the algorithm of the present study has been tested vs. several test cases. The first was by setting the amplitude's value of the waviness to zero and computing the flow characteristics inside parallel-plate channel fully filled with porous media. The computed velocity profile of fully developed region was compared with the corresponding analytical solution stated by Kaviany (1985) (see Figure 4). The second test case was by comparing the isotherms obtained by the present code with the case study that presented by Mohammad (2003) (see Figure 5). Finally, a comparison was performed between the values of the average Nusselt number at deferent values of Darcy number obtained by the current study and the two mentioned studies (Kaviany, 1985; Mohammad, 2003) (see Table 1). All the mentioned comparisons showed a good agreement.

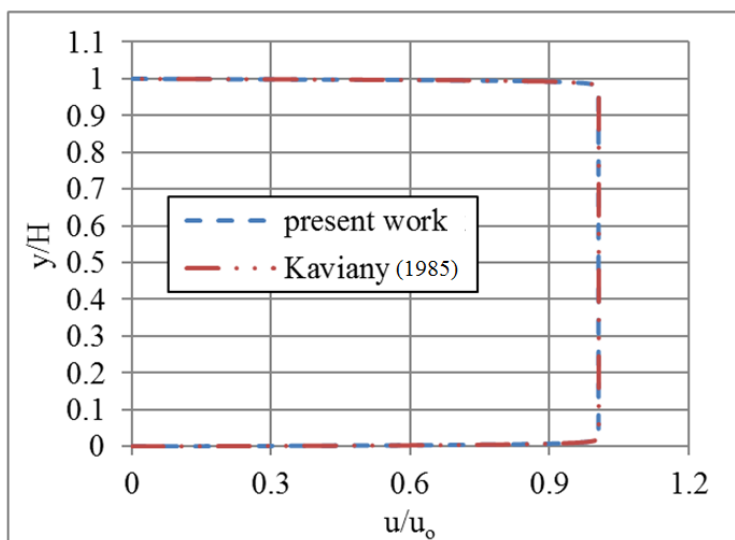


Figure 4. Comparison of the velocity profile between (a) Kaviany (1985), and (b) the present study for $Da = 10^{-5}$ and $\phi = 0.9$

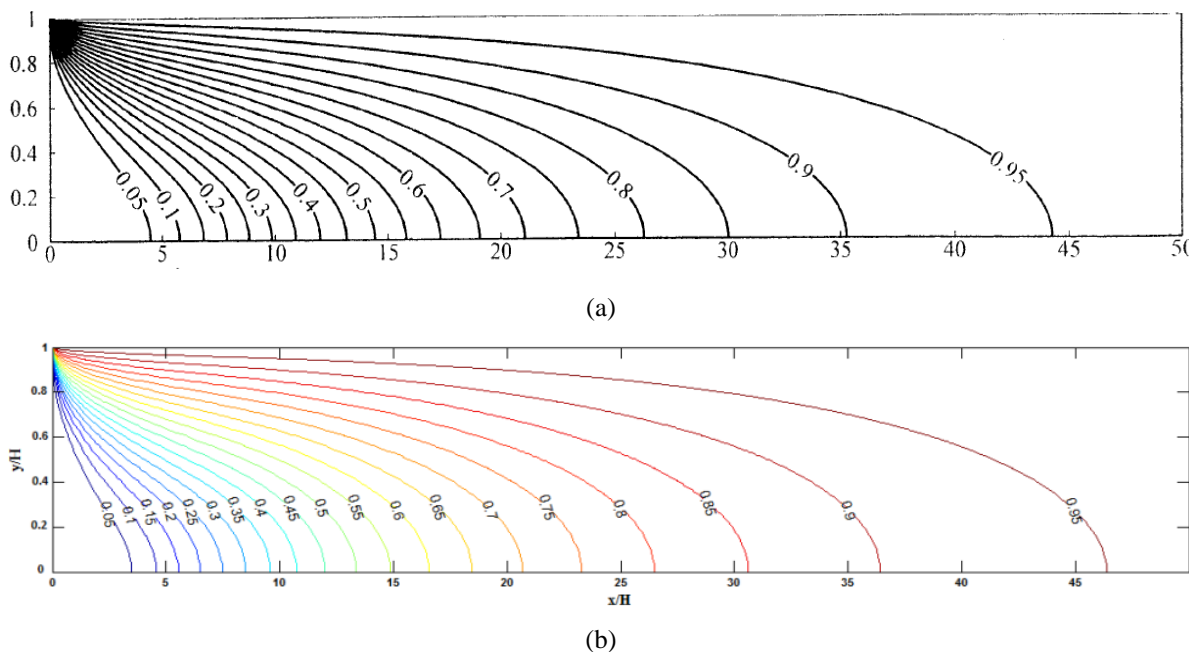


Figure 5. Isotherms comparison between (a) Mohammad (2003), and (b) the present study

Table 1. Average Nusselt number validation

Darcy No.	Kaviany (1985)	Mohammad (2003)	Present work
10^{-4}	4.880	4.8865	4.8875
10^{-5}	4.915	4.9190	4.9175
10^{-6}	4.932	4.9300	4.9350

4. Results and Discussions

4.1 The Independence of Reynolds Number

Bejan (2003) and many others like Kaviany (1985) have stated that the local Nusselt number remains constant for the thermally fully developed flow region inside a porous flat-walled channel. So, it is not affected by changing Reynolds number there, whereas this effect is clear in the entrance region. In order to determine the distance (x), from entrance section, at which the flow thermally completes its development, it is necessary to conduct a study about the dependence of Nusselt number on Reynolds number in that region and at which distance this dependence ends. Thereby, the start section of the wavy-walled part can be estimated, and the effect of waviness in the surface on Nusselt number can be purely studied.

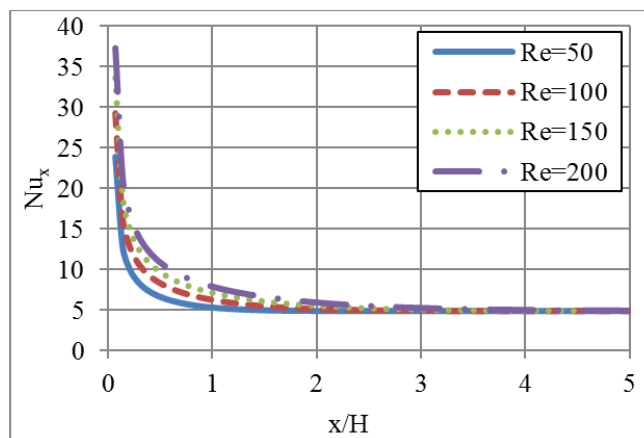


Figure 6. Local Nusselt number distribution along the surfaces of the walls for the simple duct in different values of Reynolds number. $Pr = 0.7$

It is clearly shown in Figure (6) that Reynolds number affects the values of the local Nusselt number at the entrance region of the channel, while this effect becomes non-existent after this region; because the flow becomes fully developed. Hereafter, it was possible to determine the safe value of the distance between the entrance of the channel and the position, beyond which the waviness will be installed and this distance was determined to be ($x = 10H$). The appropriate value of Reynolds number, which gives the isotherms an obvious appearance especially in remote areas from the entrance, was ($Re = 200$) for all cases of this study.

4.2 Darcy Number Effect

Generally, Darcy number strongly affects the growth of the hydraulic boundary layer. Decreasing the former significantly makes the latter forming and growing quickly. Also, the less the Darcy number, the less the boundary layer thickness. Figure (7) shows that the velocity profile at high Darcy numbers becomes similar to the profile of the flow inside non-porous channel. Moreover, going towards low Darcy numbers will reduce the velocity of fluid in the middle of the channel, and the contrast is taking place close to the surfaces. Thus, the velocity will be uniform along the distance between the upper and lower surface. In other words, the porous media affects the fluid flow inside the channel by homogenizing it.

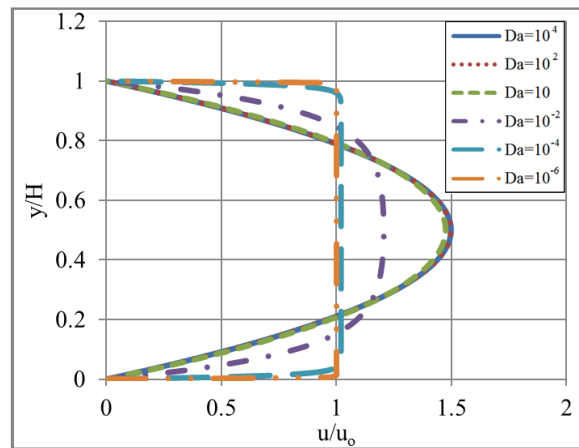


Figure 7. The fully-developed velocity profile inside simple duct for several values of Darcy number
 $Re = 200, Pr = 0.7$

Increasing the velocity of the fluid adjacent to the boundaries leads to increase the convection heat transfer there. And this exactly is the benefit of porous medium in improving the applications required more heat transfer. Figure (8) shows the velocity profile of fluid in the converging part of the wavy channel at different values of Darcy number. In this figure, it is noticed that the fluid velocity, for low Darcy numbers, is highly greater near the surfaces than it in the middle.

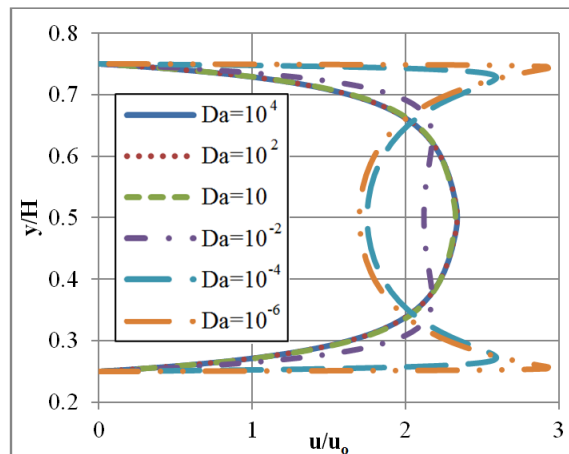


Figure 8. The fully-developed velocity profile inside wavy channel (Case A) in the convergent part for several values of Darcy number. $Re = 200, Pr = 0.7$

In this study, the value of Darcy number was selected to be ($Da = 10^{-5}$). The reason of choosing such a value is that it gives more heat transfer rate than the higher values. As well as, it clearly shows the effect of the porous medium within the region of study. On another hand, this value is more applicable than the lower values.

4.3 Effect of Porous Media on the Separation in Flow

Previous works like (Duoxing et al., 2009) had stated that the (Darcy–Forchheimer–Brinkman) equation degenerates into classical (Navier–Stokes) equation and that has the same effect at ($\phi = 0.9, Re = 200, Da = 10^4$). In the current study, two values of Darcy number were set ($Da = 10^4, Da = 10^{-5}$) in order to study the influence of porous medium existence on the separation phenomenon. Reynolds number was set to be a low constant value ($Re = 10$). The reason of choosing such a low value is to show the vortex clearly.

Figure 9(a) shows that the velocity of flow, adjacent to the wavy surface, is fluctuated in amount between maximum on peaks and minimum in bottoms. A contrary fluctuation in the amount of the local pressure

accompanies the fluctuation in velocity amount there. This flow behavior tends to the separation and circulation to occur in each furrow. The influence of the existence of porous medium can be clearly observed from Figure 9(b). Although the fluctuation in velocity and pressure amounts is not differ between the two posed cases, the separation doesn't occur and the circulation disappeared. The reason of such a behavior is that the porous medium dominates the fluid layers and partially prevents the influence between each neighboring ones. Thereby, a homogenous flow is in everywhere inside the porous medium. The relationship between the existence of porous medium and the circulation in flow is explicated by the streamlines in Figures 10 (a) and (b).

It is worth to say that the porous medium is strongly analogues, in function, to the honeycomb. The latter is typically utilized in homogenizing fluid entered the wind tunnel. Therefore, Kaffler et. al. (2003) and several other studies have already modeled the flow inside honeycomb by the equations of the flow inside porous medium.

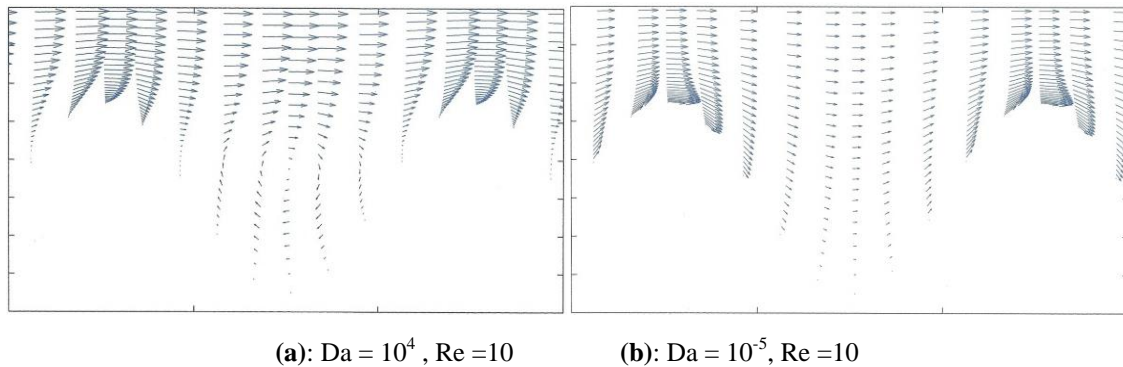


Figure 9. Velocity vectors inside wavy channel (Case A) for two different values of Darcy number. $Pr = 0.7$

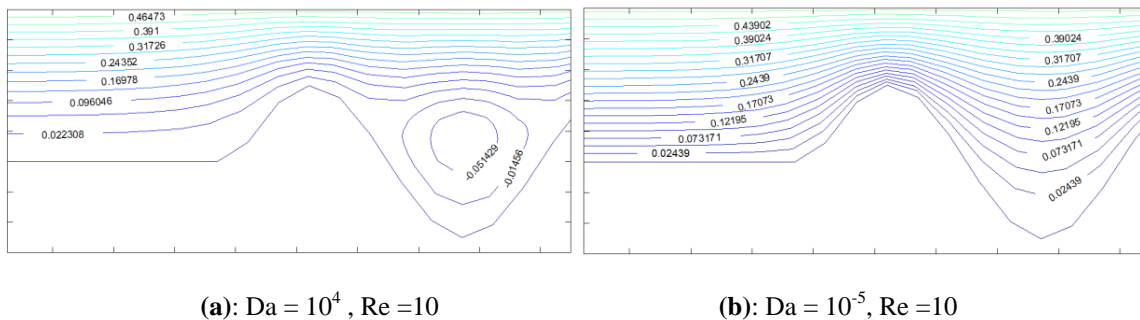


Figure 10. Streamlines contours inside wavy channel (Case A) for two different values of Darcy number. $Pr=0.7$

4.4 Flow Field

The results of the hydrodynamic characteristics are represented by velocity vectors and streamlines contours in Figures 11 and 12. Figure 11(a) shows the fully-developed velocity vectors of flow inside flat plate channel. In this figure, the most important note is the homogeneous and semi-uniform flow along the distance between the walls due to the presence of porous medium. As well as, the thin thickness of the hydraulic boundary layer.

Figure 11(b) shows the effect of waviness on the nature of flow. In this figure, it is clearly observed that the high drop in pressure, near the surface towards the peak, accelerates the particles of fluid increasing their kinetic energy. On the other hand, this drop in pressure gradually vanishes, as one is moving from the surfaces towards the depth, under the domination of porous medium. This vanishing in pressure is accompanied by decreasing the velocity variation range between the convergent and divergent parts of the channel.

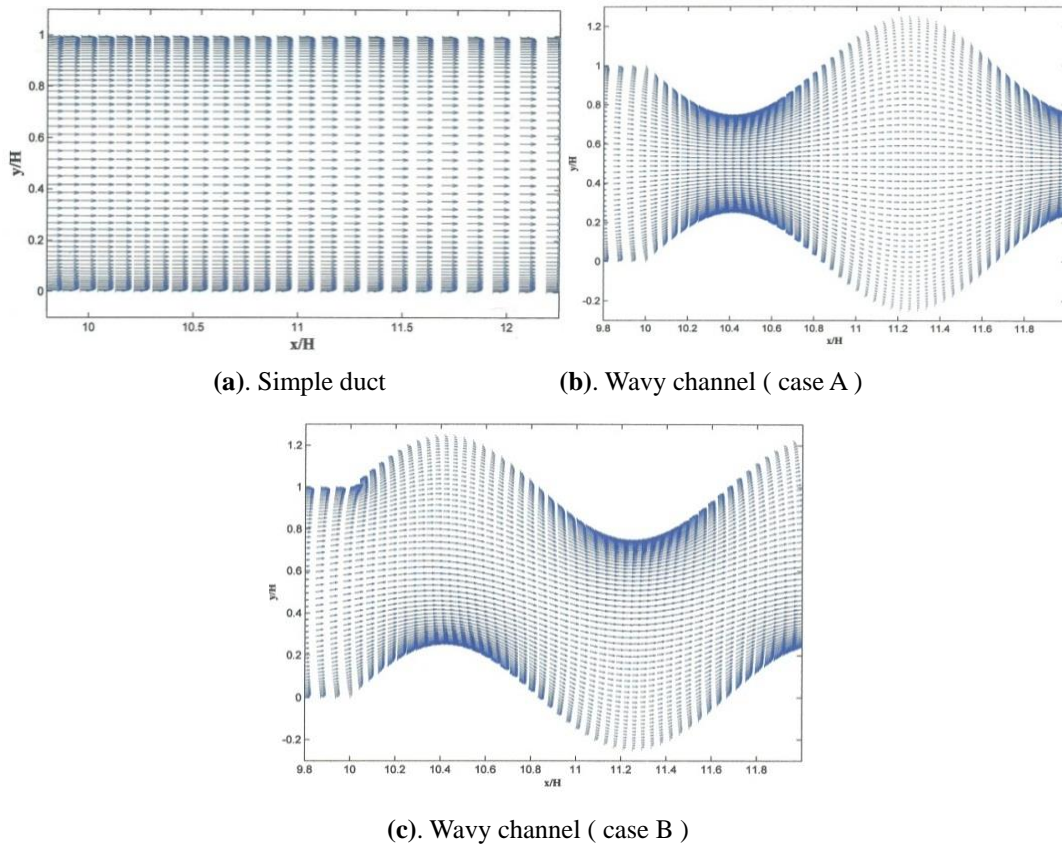


Figure 11. Velocity vectors of the flow for the three cases of present study. $Da = 10^{-5}$, $\phi = 0.9$, $Re = 200$, $Pr = 0.7$

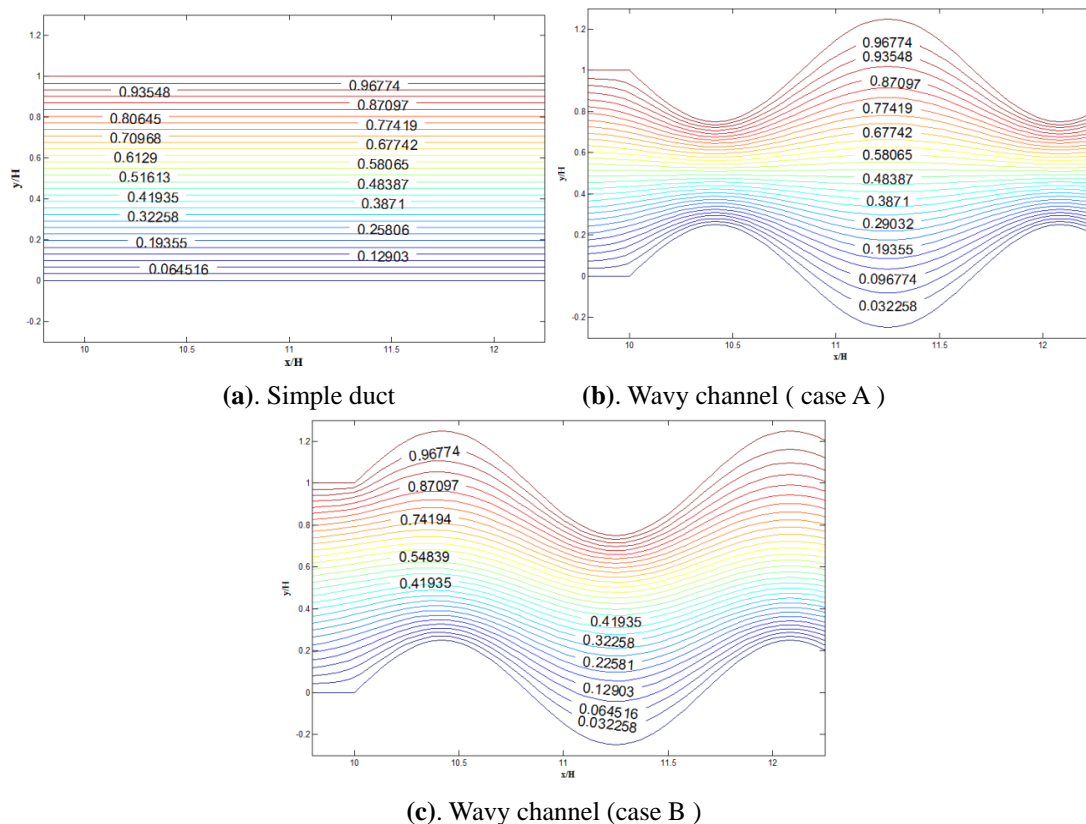


Figure 12. Streamlines contours of the flow for the three cases of present study. $Da = 10^{-5}$, $\phi = 0.9$, $Re = 200$, $Pr = 0.7$

On that basis, It is clearly noticed that the maximum velocity (at the crests) within a single velocity profile is close to the surface not in the middle of the channel. The main difference between the two cases of waviness (A & B) is that in case A there is symmetry about the longitudinal axis of the channel and this makes the fluid flowing in straight lines in the middle. Whereas, in case B (see Figure 11(c)) there is no symmetry, therefore the fluid exhibits a wavy path influenced by the waviness of the channel.

Figures (12(a), (b), and (c)) show the streamlines contours for the three cases of the current study. The most important notice in these figures that the flow is homogenous and there is no circulation due to the existence of porous medium.

4.5 Thermal Performance and Nusselt Number

Heat transfer results of the three cases in this study are presented in terms of the isotherms and local Nusselt number figures. The distribution of the local Nusselt number for the cases A & B of wavy surfaces and the simple duct case is presented in Figure 13. This figure shows that the local Nusselt number values in the furrow of the wavy wall decrease, with respect to the simple duct, and become almost zero due to the high reduction in velocity there. In contrary at the crests, one can notice that the local Nusselt number values rise sharply. The reason is that the velocity of the flow, adjacent to the surface toward the crests, is increasing until it reaches values higher than those in the depth of the channel, as aforementioned. Hence, the convection heat transfer significantly increases between the surface and the flowing fluid. It is also noticed, due the nature of the velocity fluctuation, that the decrease and increase in the local Nusselt number values weren't of the same style, where the decrease remained retracted in low rang, while the increase took a significant rise extent.

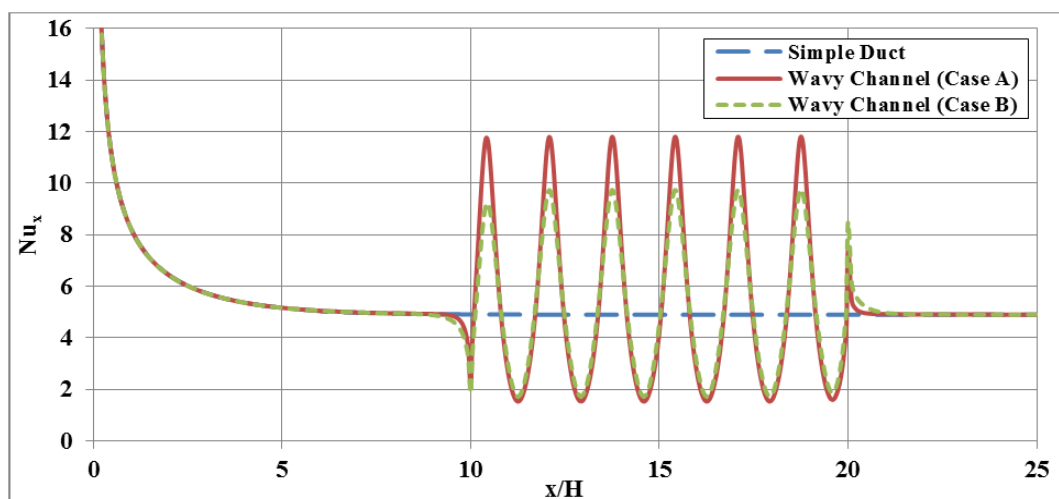


Figure 13. The distribution of the local Nusselt number for the three cases of study. $Da = 10^{-5}$, $\phi = 0.9$

Regarding the comparison between the two cases A and B. It is noticed that the rise in the local Nusselt number at the crests had a greater extent of increase incase A than it had in case B. This leads to conclude that case A gives a larger increase in the heat transfer rate than case B. On another hand, by comparing these two cases with the simple channel it is found that the waviness in the surfaces has already enhanced the heat transfer (see Table 2).

It is worth to mention that the thermal fully developing length decreased due to the presence of the waviness in the surfaces as comparing to the simple duct (see Figure 14). This observation confirms the conclusion that the thermal performance of the wavy channel is better than the straight channel (simple duct).

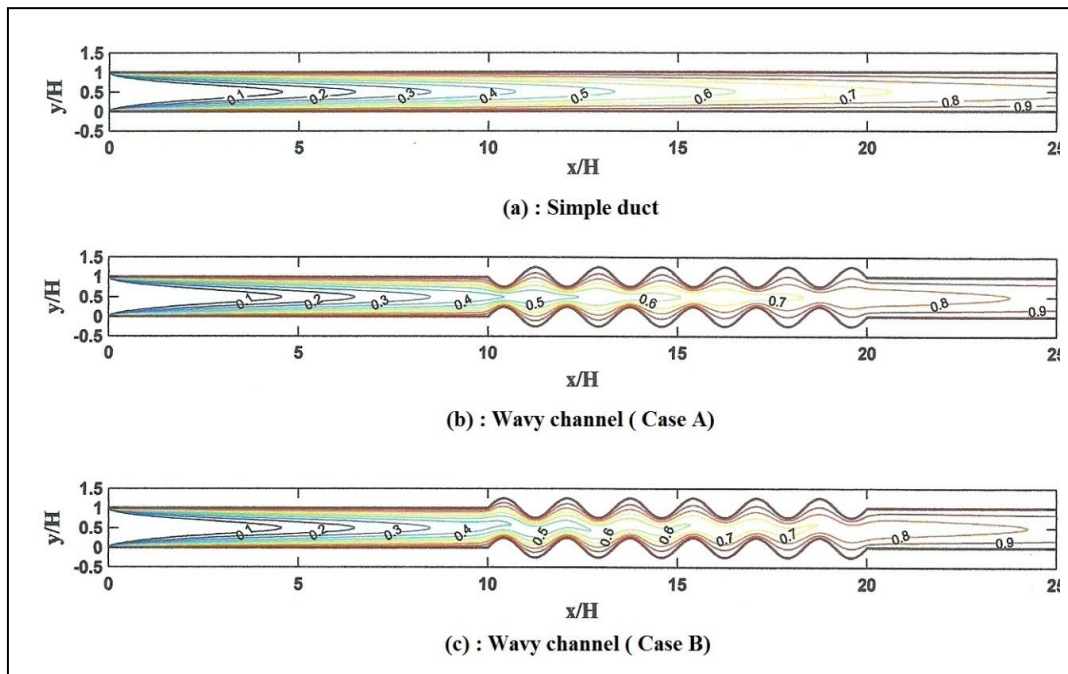


Figure 14. Isotherms contours for the three cases of study. $Da = 10^{-5}$, $\phi = 0.9$

Table 2. Average Nusselt number, amounts and percentage of increase for cases A & B in comparing with the simple duct. $Da = 10^{-5}$, $\phi = 0.9$, $Re = 200$, $Pr = 0.7$

Case	Nu	% increment
Simple duct	4.924	---
Wavy channel (case A)	5.4212	10.097
Wavy channel (case B)	5.1499	4.587

5. Conclusions

A numerical study was performed to investigate the combined effect of waviness and porous media on the convection heat transfer and fluid flow characteristics. This study assumed two models of wavy channel fully filled with porous medium. The comparison between these models and simple duct had been discussed. The main conclusions of this study can be summarized as follows:

- 1) For low Darcy numbers, It is clearly noticed that the maximum velocity, at the crests of wavy surfaces, within a single velocity profile is close to the surface not in the middle of the channel.
- 2) Porous medium dominates the fluid layers and partially prevents the influence between each neighboring ones. Thus, the separation doesn't occur and the circulation, in the cavities of wavy surfaces, disappeared. Thereby, a homogenous flow is in everywhere inside the porous medium.
- 3) The increase and decrease in local Nusselt number values for the wavy channel weren't of the same style, where the decrease (in the furrows) remained retracted in low rang, while the increase (in the crests) took a significant rise extent.
- 4) The symmetric converging-diverging channel (case A) gives more enhancement in heat transfer than the channel with concave-convex walls (case B). However, the thermal performance of the wavy channels (cases A & B) is better than the straight channel (simple duct).

Further investigations about the effects of wave length, amplitude, and phase change of the wavy surfaces on the fluid and thermal characteristics are required.

Acknowledgments

The authors acknowledge the support of Mechanical Engineering Department in Mosul University.

References

- Angirasa, D. (2002). Experimental Investigation of Forced Convection Heat Transfer Augmentation with Metallic Fibrous Materials. *Int. J. Heat Mass Transfer*, 45, 919-922. [http://dx.doi.org/10.1016/S0017-9310\(01\)00196-X](http://dx.doi.org/10.1016/S0017-9310(01)00196-X)
- Bejan, A., & Kraus, A. D. (2003). *Heat Transfer Handbook*. Hoboken, New Jersey, USA: John Wiley & Sons, Inc.
- Duoxing, Y., Yang, Y., & Costa, V. A. F. (2009). Numerical Simulation of Non-Darcian Flow Through a Porous Medium. *Particuology*, 7, 193-198. <http://dx.doi.org/10.1016/j.partic.2009.02.001>
- Hadim, H., & North, M. (2005). Forced Convection in a Sintered Porous Channel with Inlet and Outlet Slots. *Int. J. Thermal Sciences*, 44, 33-42. <http://dx.doi.org/10.1016/j.ijthermalsci.2004.04.016>
- Kaffler, J., Ortega, A., & Bouldin, B. (2003). Experimental Measurement of Boundary Layer Flow Suction into a Honeycomb Panel, ASME, *International Mechanical Engineering Congress and Exposition (IMECE)*, Washington, USA.
- Kaviany, M. (1985). Laminar Flow Through a Porous Channel Bounded by Isothermal Parallel Plates. *Int. J. Heat Mass Transfer*, 28(4), 851-858. [http://dx.doi.org/10.1016/0017-9310\(85\)90234-0](http://dx.doi.org/10.1016/0017-9310(85)90234-0)
- Kim, S. Y., Kang, B. H., & Kim, J.-H. (2001). Forced Convection from Aluminum Foam Materials in an Asymmetrically Heated Channel. *Int. J. Heat Mass Transfer*, 44, 1451-1454. [http://dx.doi.org/10.1016/S0017-9310\(00\)00187-3](http://dx.doi.org/10.1016/S0017-9310(00)00187-3)
- Middlecoff, J. F., & Thomas, P. D. (1980). Direct Control of The Grid Point Distribution in Meshes Generated by Elliptic Equation. *AIAA Journal*, 18(6), 652-656. <http://dx.doi.org/10.2514/3.50801>
- Mohammad, A. A. (2003). Heat Transfer Enhancements in Heat Exchangers Fitted with Porous Media Part I: Constants Wall Temperature. *Int. J. Thermal Sciences*, 42, 385-395. [http://dx.doi.org/10.1016/S1290-0729\(02\)00039-X](http://dx.doi.org/10.1016/S1290-0729(02)00039-X)
- Petrović, Z., & Stupar, S. (1996). *Computational Fluid Dynamics I*. Mechanical Engineering Faculty, University of Belgrade, Belgrade, Serbia.
- Russ, G., & Beer, H. (1997a). Heat Transfer and Flow Fluid in a Pipe with Sinusoidal Wavy Surface—I. Numerical Investigation. *Int. J. Heat Mass Transfer*, 40(5), 1061-1070. [http://dx.doi.org/10.1016/0017-9310\(96\)00158-5](http://dx.doi.org/10.1016/0017-9310(96)00158-5)
- Russ, G., & Beer, H., (1997b). Heat Transfer and Flow Fluid in a Pipe with Sinusoidal Wavy Surface—II. Experimental Investigation. *Int. J. Heat Mass Transfer*, 40(5), 1071-1081. [http://dx.doi.org/10.1016/0017-9310\(96\)00159-7](http://dx.doi.org/10.1016/0017-9310(96)00159-7)
- Saniei, N., & Dini, S., (1993). Heat Transfer Characteristics in a Wavy-Walled Channel. *ASME*, 115, PP.788-792. <http://dx.doi.org/10.1115/1.2910756>
- Stone, K. M., & Vanka, S. P. (1999). Numerical Study of Developing Flow and Heat Transfer in Wavy Passages. *ASME J. Fluid Eng.*, 121, 713-719. <http://dx.doi.org/10.1115/1.2823528>
- Tanda, G., & Vittori, G. (1996). Fluid Flow and Heat Transfer in a Two-Dimensional Wavy Channel. *Int. J. Heat Mass Transfer*, 31, 411-418. <http://dx.doi.org/10.1007/s002310050077>
- Vafai, K., & Tien, C. L. (1981). Boundary and Inertia Effects on Flow and Heat Transfer in Porous Media. *Int. J. Heat Mass Transfer*, 24, 195-203. [http://dx.doi.org/10.1016/0017-9310\(81\)90027-2](http://dx.doi.org/10.1016/0017-9310(81)90027-2)
- Van der Sman, R. G. M. (2002). Prediction of Airflow Through a Vented Box by The Darcy-Forchheimer Equation. *Journal of Food Engineering*, 55, 49-57. [http://dx.doi.org/10.1016/S0260-8774\(01\)00241-2](http://dx.doi.org/10.1016/S0260-8774(01)00241-2)
- Wang, C.-C., & Chen, C.-K. (2002). Forced Convection in a Wavy-Wall Channel. *Int. J. Heat Mass Transfer*, 45, pp. 2587-2595. [http://dx.doi.org/10.1016/S0017-9310\(01\)00335-0](http://dx.doi.org/10.1016/S0017-9310(01)00335-0)
- Xie, G.-N., Wang, Q.-W., Zeng, M., & Luo, L.-Q. (2007). Numerical Investigation of Heat Transfer and Fluid Flow Characteristics inside a Wavy Channel. *Heat Mass Transfer*, 43, 603-611. <http://dx.doi.org/10.1007/s00231-006-0133-7>

Copyrights

Copyright for this article is retained by the author(s), with first publication rights granted to the journal.

This is an open-access article distributed under the terms and conditions of the Creative Commons Attribution license (<http://creativecommons.org/licenses/by/3.0/>).